The Fourth International Workshop on
Micro and Nanotechnology for Power Generation
and Energy Conversion Applications
PowerMEMS 2004
November 28 - 30, 2004
Kyoto, Japan

Fuel and Air Supply System using an Ejector for Microcombustors

Daisuke Satoh[1], Shuji Tanaka[1], Masayoshi Esashi[2]
[1]Department of Nanomechanics, Tohoku University
6-6-01 Aoba, Aramaki-aza, Aoba-ku, Sendai, Miyagi 980-8579, Japan
Tel +81-22-217-6937, Fax +81-22-217-6935, E-mail sato@mems.mech.tohoku.ac.jp
[2]New Industry Creation Hatchery Center, Tohoku University
6-6-01 Aoba, Aramaki-aza, Aoba-ku, Sendai, Miyagi 980-8579, Japan

Abstract

This paper compares the results of CFD (computational fluid dynamics) simulation and experimental results of a MEMS-based ejector, which has been developed to supply fuel-air mixture to microcombustors. The CFD results showed fair agreement with experimental results, when fuel supply pressure was in a practical range (> 200 kPa). From the pressure distribution near the nozzle, it was confirmed that a negative pressure was generated by the supersonic jet of fuel from a Laval nozzle. From the velocity distribution near the outlet, a slow reverse flow was observed, and it was found that the mixed flow was not fully developed in the mixing section. From the result, it is concluded that the developed ejectors leave plenty of room for improvement by CFD simulation.

Keywords: Ejector, Combustor, CFD, negative pressure

1 INTRODUCTION

Portable power sources need higher and higher energy density due to increasing functions and longer operation time of portable devices. The energy density of a lithium-ion battery, which is the best existing secondary battery, is as high as 200 Wh/l and 150 Wh/kg. But a lithium-ion battery is approaching its theoretical limit.

Hydrocarbon fuels such as methanol and gasoline have much more chemical energy than the electrical energy in batteries with the same volume. Therefore, miniature power sources using hydrocarbon fuels have recently been under development to answer the increasing energy demand of portable devices[1-3].

For portable information devices such as laptop computers and video camcoders, direct methanol fuel cells (DMFC) are receiving significant attention. However, DMFCs suffer from a low power density, so that it occupies considerable volume in systems.

For high power density applications like self-powered small robots, the low power density of the DMFC is a serious problem. However, a polymer electrolyte fuel cell (PEFC) using hydrogen as fuel has one order of magnitude higher power density compared to DMFCs, but hydrogen is problematic in terms of storage, refueling infrastructure and explosion hazard. Therefore, fuel reforming to convert hydrocarbon into hydrogen at microscale is attractive especially for high power density applications[4, 5].

MEMS-based ejectors[6] has been developed during this research to supply fuel-air mixture to a microcombustor, which is one of the components of fuel reformers, thermophotovoltaic generators[7, 8] and thermoelectric generators[9, 10]. In this paper, the results of computational fluid dynamics (CFD) simulation for a MEMS-based ejector are presented.

2 STRUCTURE

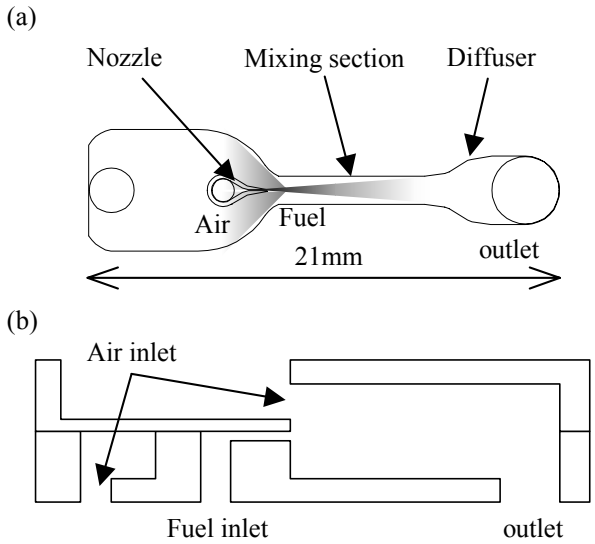

Fig. 1 Structure of the MEMS-based ejector

Figure 1 illustrates the structure of the MEMS-based ejector. The ejector is composed of a nozzle, mixing section and diffuser. The size of the flow channel shown in Fig.1 (a) is approximately 21 mm × 5 mm × 1 mm (length × width × height). The nozzle is a Laval nozzle, whose throat width and divergence half-angle are 23.5 μm and 15 °, respectively. Fuel (primary flow) is ejected from a nozzle at supersonic velocity, and air (secondary flow) is sucked by negative pressure and viscous dragging generated by the jet of the primary flow. Fuel and air are mixed in a mixing section,

and the mixed flow return its static pressure at a diffuser.

Figure 1 (b) shows the cross section of the MEMS-based ejector. The mixing section is about 1024 μm deep, while the nozzle is 25 μm deep. From theoretical calculation and previous experimental results[6], it is found that the ratio of the cross sectional area of the mixing section to that of the nozzle, is called the cross sectional area ratio, is one of key design parameters which determine the performance of the ejector. The flow channels are fabricated on a silicon substrate by 2-step deep reactive ion etching. The etched substrates are directly bonded to seal the flow channel.

3 PREVIOUS RESULTS AND PURPOSE OF THIS STUDY

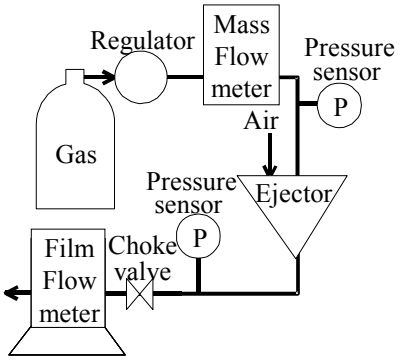

Fig.2. Experimental setup

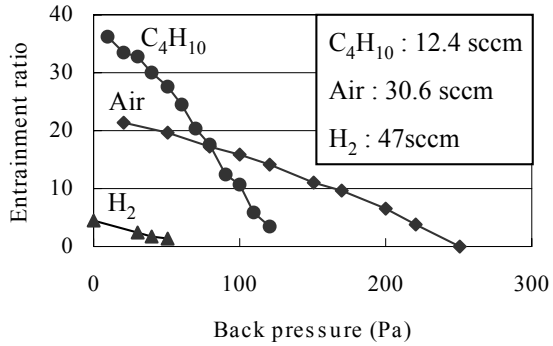

Fig.3 Relationship between back pressure and entrainment ratio

In the previous study, MEMS-based ejectors were fabricated and tested. Figure 2 is the experimental setup. In the previous study, the primary flow gases were C_4H_{10}, air or H_2. The pressure of the primary flow was 182 (C_4H_{10}), 376 (air) or 100 kPa (H_2). Figure 3 shows the relationship between back pressure and entrainment ratio which is defined bellow. The back pressure is gauge pressure at the outlet of the ejector, and the entrainment ratio is defined as the ratio of the mass flow rate of the secondary flow to that of the primary flow.

The entrainment ratio required for the complete combustion of C_4H_{10} is more than 31. When the back pressure is under 30 Pa, the entrainment ratio satisfies this requirement. However, the pressure loss of microcombustor is generally more than 30 Pa. For example, a MEMS-based butane combustor which we have developed for thermoelectric generation has a pressure loss of 184 Pa at the same flow rate (394 sccm)[10]. Thus, for practical applications, the performance of the microcombustor must be improved especially in terms of back pressure resistance.

The purpose of this study is to find a solution of this problem by investigating flow inside the ejector. The direct observation of the flow inside the ejector is difficult, because it is small and sealed with a silicon substrate. Thus, in this study, we analyzed flow in the ejector by CFD simulation.

4 COMUPUTATIONAL SIMULATION

4.1 Analysis model

Figure 4 is modeled only one forth of the ejector. The solution was processed by FLUENT, assuming that the flow was viscous and laminar flow, and that the fluid was air regarded as compressible ideal gas. As boundary conditions, the wall temperature was set at 300 K, and total pressure of fuel inlet and static pressure of the outlet were given. The total pressure of the air inlet is atmospheric, and that at the fuel inlets was changed from 50 kPa to 400 kPa.

The size of the nozzle is 30 μm × 25 μm (width × height). The width of the throat of the Laval nozzle is 23.5 μm. The size of the mixing section is 9310 μm × 1330 μm × 1024 μm (length × width × height). The angle of the diffuser is 22 º.

4.2 Comparison between experimental results and CFD results

Figure 5 shows the relationship between the primary pressure (Air) and entrainment ratio. The static pressure at the outlet is atmospheric. When the primary pressure is high, the CFD results are close to the experimental results. When the primary pressure is low, however, the CFD results and the experimental results show considerable difference.

It is believed, the pressure loss at the film flow meter and connections shown in Fig. 3 were the major reason for the

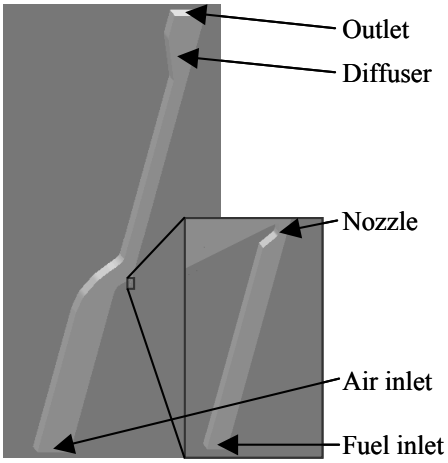

Fig.4 The analysis model

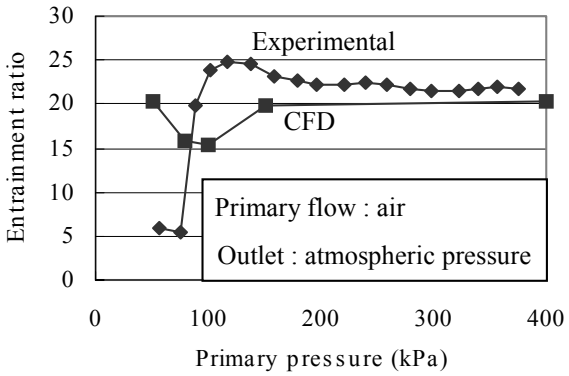

Fig.5 Relationship between primary pressure and entrainment ratio

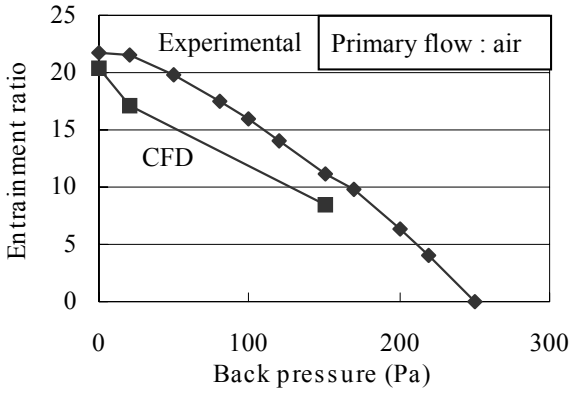

Fig. 6 Relationship between back pressure and entrainment ratio

difference. The calculated pressure loss at the film flow meter and connections based on the experimental results in the previous study, was 1.7 Pa at a flow rate of 59.7 sccm. This is not large enough to explain the difference.

When the primary pressure is approximately below 100 kPa, the jet of the primary flow from the nozzle becomes subsonic. So, the case of low primary pressure will be calculated again assuming that the flow is incompressible ideal gas.

Figure 6 shows Relationship between back pressure and entrainment ratio. The primary pressure of the experiment is 376 kPa in the experiment and 400 kPa in the CFD simulation. The experimental result and CFD result show a similar tendency that entrainment ratio decreases with increasing back pressure.

The CFD results show fair agreement with experimental results, when the primary pressure is in a practical range (> 200 kPa). Consequently, the CFD simulation seems useful to design the ejector.

4.3 Static pressure around the nozzle

The static pressure distribution around the nozzle is shown in Fig.7. The boundary conditions used are follows,

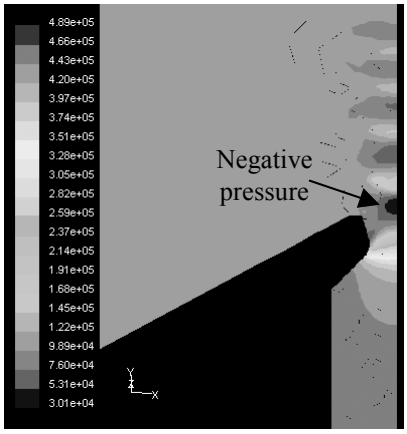

Fig.7 Static pressure around the nozzle (primary pressure is 400 kPa)

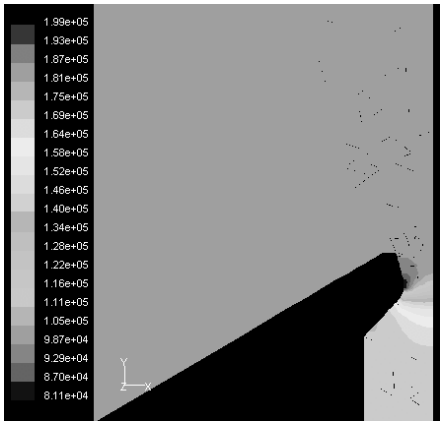

Fig.8 Static pressure around the nozzle (primary pressure is 100 kPa)

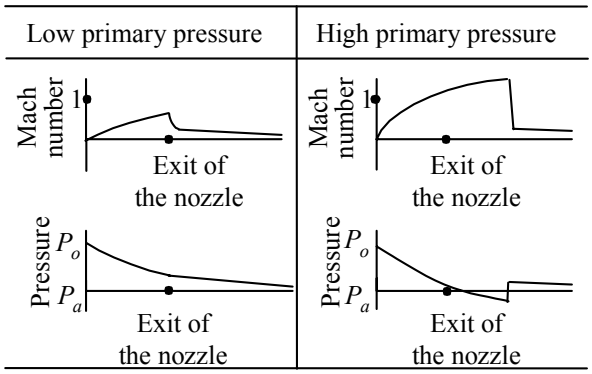

Fig.9 Pressure and Mach number around the nozzle

the primary pressure is set at 400 kPa, and static pressure at the outlet is set atmospheric pressure. It was found that a negative pressure appears around the exit of the nozzle. Figure 8 shows static pressure distribution around the nozzle when the primary pressure is 100 kPa. In this case, negative pressure is not generated. The Laval nozzle is designed as the primary flow is correctly expanded when the primary pressure is 350 kPa. When the primary pressure is 400 kPa, the pressure of primary flow becomes about 300 kPa at nozzle. Therefore, the primary flow is over expanded.

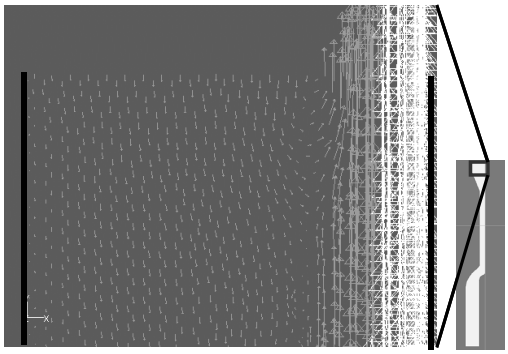

Fig.10 Velocity vectors near the outlet (primary pressure is 400 kPa)

However, when the pressure of the primary flow is 100 kPa, the pressure becomes about 60 kPa at nozzle. So, this pressure is not enough to generate negative pressure. Figure 9 schematically compares the cases of high and low primary pressure on pressure and Mach number around the nozzle.

4.4 Flow near the outlet of the ejector

Figure 10 shows the velocity vectors near the outlet. The primary pressure is 400 kPa, and the static pressure at the outlet is atmospheric. Similar results are obtained on other boundary conditions. Near the center of the flow channel, flow is heading for the outlet at relatively high velocity. In the other part of the flow ways, however, slow reverse flow is observed. Also, the mixed flow is not fully developed in the mixing section. From this result, it is clear that the design of the mixing section and the diffuser should be improved. By CFD simulation, it should be possible to find a solution under the limitation of back pressure and size.

5 DISCUSSION

When the primary flow is supersonic, the velocity of the primary flow is constant. However, the negative pressure is dependent on the primary pressure. From the results of experimental and CFD simulation, variation of the entrainment ratio has little affect when the primary flow is supersonic flow. Therefore, the reason of rapid increasing of the experimental results is not explained fully by negative pressure.

6 CONCLUSION

A MEMS-based ejectors to supply fuel-air mixture to microcombustors has been developed. They have the problem that they cannot supply enough air when pressure at the outlet becomes more than a few tens Pa. To solve the problem, CFD simulation was conducted. In this study, the CFD results were compared to experimental results to verify the CFD results. Consequently, The CFD results showed fair agreement with experimental results, when fuel supply pressure was in a practical range (> 200 kPa).

From pressure distribution near the nozzle, it was confirmed that negative pressure was generated by the supersonic jet of fuel from a Laval nozzle. From velocity distribution near the outlet, slow reverse flow was observed, and it was found that the mixed flow was not fully developed in the mixing section. From this result, the developed ejectors leave plenty of room for improvement by CFD simulation.

ACKNOWLEDGEMENTS

This work was supported by the New Energy and Industrial Technology Development Organization (NEDO) of Japan. Daisuke Satoh was supported by Research Fellowships of the Japan Society for the Promotion of Science for Young Scientists.

REFERENCES

[1] A. H. Epstein *et al*., Micro-Heat Engines, Gas Turbines, and Rocket Engines ―The MIT Microengine Project―, Proc. 28th AIAA Fluid Dynamics Conference, 4th AIAA Shear Flow Control Conference (1997) AIAA97-1773.

[2] P. Kang *et al*., Micro Turbocharger on a Single Silicon Rotor Proceedings of ASME Turbo Expo 2004, Power for Land, Sea, and Air (2004) GT-2004-53565.

[3] Shuji Tanaka *et al*., Turbo test rig with hydroinertia air bearings for a palmtop gas turbine, J. Micromech. Microeng, 14, No 11 (2004) 1449-1454.

[4] Jamelyn D. Holladay *et al*., Microfuel processor for use in a miniature power supply, J. Power Sources, 108 (2002) pp. 21-27.

[5] Kuei-Sung Chang *et al*., MEMS-based fuel reformer with suspended membrane structure, IEEJ Trans. SM, 123 (2003) 346-350.

[6] Daisuke Sato *et al*., A Micro-Ejector for A Micro-Combustor, Proc. The 20th Sensor Symposium (2003) 359-364.

[7] W. M. Yang *et al*., Development of microthermophotovoltaic system, Appl. Phys. Lett., 81 (2002) 5255-5257.

[8] Ole M. Nielsen *et al*., A THERMOPHOTOVOLTAIC MICRO-GENERATOR FOR PORTABLE POWER APPLICATIONS, Digest of Technical Papers, Transducers '03 (The 12th International Conference on Solid-State Sensors, Actuators and Microsystems) (2003) 714-717.

[9] Chunbo Zhang *et al*., An Integrated Combustor-Thermoelectric Micro Power Generator, Digest of Technical Papers, Transducers '01, Eurosensors XV (The 11th International Conference on Solid-State Sensors and Actuators) (2001) 34-37.

[10] Kazushi YOSHIDA *et al*., HIGH ENEGY DENSITY MINIATURE ELECTRICAL AND THERMAL POWER SOURCE USING CATALYTIC COMBUSTION OF BUTANE, Technical Digest, 17th IEEE International Conference on Micro Electro Mechanical Systems (2004) 316-321.